AUT Journal of Electrical Engineering

AUT J. Elec. Eng., 51(2) (2019) 113-122
DOI: 10.22060/eej.2019.15276.5257

General Linear Chirplet Transform and Radar Target Classification

R. Amiri[1*], A. Shahzadi[2]

[1] Technical and Engineering Faculty, South Tehran Branch, Islamic Azad University, Tehran, Iran.
[2] Technical and Engineering Faculty, Semnan University, Semnan, Iran.

ABSTRACT: In this paper, we design an attractive algorithm aiming to classify moving targets including human, animal, vehicle and drone, at ground surveillance radar systems. The non-stationary reflected signal of the targets is represented with a novel mathematical framework based on behavior of the signal components in reality. We further propose using the generalized linear chirp transform for the analysis stage. To enhance the classification performance, the rotation invariant pseudo Zernike-Moments are extracted from the time-frequency map. Consequently, the obtained features are trained to the k-NN classifier. In the numerical experiments we show the superiority of the proposed method in comparison with the existing recent counterparts, for both performance as well as the computational complexity. The results indicate that the proposed method obtains the rate of 95% accuracy in classification performance, when the signal to noise ratio is higher than 25dB. Index Terms—Automatic Target Recognition (ATR), General Linear Chirplet Transform (GLCT), Moving Target Detector (MTD), Radar Target Classification, Short Time Fourier Transform (STFT).

Review History:
Received: 2018-11-12
Revised: 2019-03-23
Accepted: 2019-04-01
Available Online: 2019-12-01

Keywords:
Automatic Target Recognition (ATR)
General Linear Chirplet Transform (GLCT)
Moving Target Detector (MTD)
Radar Target Classification

I. Introduction

A. Overview

Ground surveillance radar systems, use narrow-band waveforms (low-resolution) for detection and tracking [1], while many target classification or identification algorithms, requires high resolution [2]–[5]. However, recent researches indicate that poor-resolution Moving Target Indication (MTI) radar systems can be used in classification of moving targets through observing the micro Doppler signatures of the reflected signal [6]–[9]. In fact, a rotating propeller on a fixed-wing aircraft, the multiple spinning rotor blades of a helicopter, or an Unmanned Aerial Vehicle (UAV); the vibrations of an engine shaking a vehicle; an antenna rotating on a ship; the flapping wings of birds; the swinging arms and legs of a walking person; and many other sources are the source of micromotion, are known as the micro-Doppler, and can be used for target classification and reduction of the sensor false alarm rate[1] [7].

MTI radar systems can reject fixed clutter through a subtraction process while remaining the moving targets. To perform this subtraction, it is necessary to keep transmit and receive parameters (i. e., operating frequency, duty cycle, intra pulse modulation, etc.) fixed for a while, and obtain Coherent Pulse Interval (CPI) [10]. Conventional Moving Target Detector (MTD) radar systems, usually use a filter-bank implemented via Fast Fast Fourier Transform (FFT) to process the reflected signal from the targets coherently, at the receive side (and profit both clutter cancellation and coherent processing gain). In low-resolution radar systems, the intra pulse modulation of the transmit waveform has not a significant effect on MTI/MTD performance when it repeats pulse-to-pulse, which is of course necessary for the MTI/MTD process. Performing FFT in slow-time and estimation of the reflected signal periodogram, can extract the micro Doppler, which can be used as the classification feature. In conventional MTI/MTD radar systems, the slow-time Doppler signal usually is converted to sound, and expert operators can identify targets by hearing the Doppler [10], [11]. But when number of target categories increases (e. g., human, animal, motorcycle, car, truck, drone, train, etc.), artificial intelligence maybe more useful than human experience and cause to decrease in classification error rate.

B. Literature Review

When we have a moving target reflecting a signal, naturally the Doppler effect comes into picture; the received signal becomes non-stationary with respect to its spectral content, even if the generated signal is stationary [12]. This nonstationarity

1- Confuser detections, such as birds for UAVs or animals for humans, can be interpreted as false alarms for a sensor system, so using the available micro-Doppler returns for classification can significantly reduce the sensor false alarm rate, thereby improving the utility of the sensor system.

*Corresponding author's email: amiri.reza61@ieee.org

in the signal provides information about the motion of the source. There are lots of literatures studying micro-Doppler characteristics through different Time Frequency (TF) analysis on target reflected signal (see [6]–[9], [11], [13]–[16] and references therein).

The conventional method typically use the Short Time Fourier Transform (STFT) and considered squared absolute value of the STFT (called the spectrogram) as an image where every point of instantaneous frequency is a pixel (see [13] and references therein). Then, through some image processing techniques, the TF plane of the target served as the inputs to the automatic target recognition (ATR) algorithms [6], [13], [17]. This methodology seems strong enough and many references have provided its powerfulness. However, extending the analysis domain beyond time and frequency gives a redundant representation of the signal which can improve the results for a classification algorithm [18].

Gabor Transform (GT) which is a special case of STFT with a tractable Gaussian window, Wavelet Transform (WT) which performs translation and dilation on signals to give high-frequency resolution, Wigner's Distribution Function (WDF) which is a Fourier transformed autocorrelation function with time averaging and time lags, Chirplet Transform (CT) that might be considered a generalization of STFT and WT where involves a complex function of time, frequency, scale and chirp rate; are some examples of TF representation for non-stationary signals [12], [19]–[23].

Recently, the newly developed deep learning algorithms are also applied to perform target classification in radar systems [24]–[28]. However, these approaches need to the selection of raw vectors with lots (millions) of trials [29]. Also, in order to perform the classification techniques and in fact, extracting feature from the micro-Doppler raw signals, they demand a relatively long time, compared with the conventional methods.

C. Contributions

In this paper, we provide a new mathematical model for micro-Doppler signature of different typical targets, including human, animal, vehicle and drone. Then, we examine effects of different TF presentation of the modelbased signals, on a designed classification algorithm. Specifically we survey how STFT and General Linear Chirplet Transform (GLCT) affect the classification performance when a model based system is employed at different situation and SNRs. The main contributions of this proposal can be enumerated as follows:

- In the present work, we first show that the Doppler signal can be modeled as a multi-component function around the cross-over time instant and then estimate its parameters from the intercepts of linear functions.
- Since we model the mirco-Doppler as a multicomponent function around the main Doppler, we can use the GLCT to estimate the Doppler and hence the source parameters.
- We show the improvements that can be achieved by an accurate TF estimation on the classification performance.

D. Organization and Notation

The rest of this work is organized as follows. In Section II, the design problem is formulated. In Section III, we develop the mathematical calculation of STFT and GLCT to deal with the problem. Section IV provides several numerical experiments to verify the effectiveness of the classier. Finally, Section V concludes the paper. The following notation is adopted in the paper. Bold lowercase letters for vectors and bold uppercase letters for matrices. The transpose, the conjugate, and the conjugate transpose operators are denoted by the symbols $(.)^{\mathbf{T}}$, $(.)^{*}$ and $(.)^{\mathbf{H}}$ respectively. The letter ȷ represents the imaginary unit (i.e., ȷ = √-1). For any $x \in \mathrm{C}$, |x| and arg (x) represent the modulus and the argument of x, respectively.

II. Signal Model

Let $\mathbf{x} \in \mathbf{C}^{\mathbf{N}}$ be the discrete time reflected signal from a point target, contaminated with clutter $\mathbf{c} \in \mathbf{C}^{\mathbf{N}}$ and white gaussian noise $w \in C^{N}$ $\boldsymbol{w} \in \mathrm{C}_{N}$ with zero mean and variance σ2. The n-th sample of the received baseband signal is [10],

$$\mathbf{x}[\mathrm{n}] = \mathbf{s}[\mathrm{n}] + \mathbf{c}[\mathrm{n}] + \mathbf{w}[\mathrm{n}], \tag{1}$$

where n = 1, . . . , N with N stands for number of pulses in CPI. The received signal passes from MTI filter to suppress clutter and improve Signal to Clutter Ratio (SCR). In this paper, without loss of generality we assume that the residual clutter is small enough and can be disregarded. The n-th sample of the received signal, after match filtering and at the output of the MTI filter is,

$$\mathbf{x}[\mathrm{n}] = \mathbf{s}[\mathrm{n}] + \boldsymbol{\nu}[\mathrm{n}], \tag{2}$$

where $\boldsymbol{\nu} \in \mathbf{C}^{\mathbf{N}}$ based on central limit theorem[1], is approximated by a zero mean colored Gaussian process of variance σ^2 whose real and imaginary components are identically distributed. Signal modeling basically can be done through two methods [1], [15]; as a stochastic process, or as the assumption of a deterministic structure but with unknown parameters. Although both approaches describe random processes, but the latter uses more information about some signal characteristics (for example, a sinusoidal signal) and can be compatible more accurately with real signatures. Regarding to the second approach, microDoppler motion mathematically can be written as,

$$\boldsymbol{s_i}[n] = a_i(n) \times exp\{\jmath a_i n^2 + \jmath 2\pi\beta_i n + \jmath 2\pi\zeta_i \cos(2\pi\mu_i n + \theta_i) + \jmath\psi_i\} \tag{3}$$

where $\mathrm{a_i(n)}$ is the amplitude of the reflected signal from the i-th scatterer of the target, α_i is the rate change of the Doppler frequency in a CPI, $\boldsymbol{\beta}_i$ is Doppler frequency of the bulk motion, $\boldsymbol{\zeta}_i$ the micromotion spatial displacement of the i-th scatterer, $\boldsymbol{\mu}_i$ is the micromotion frequency of the i-th scatterer, θ_i is the initial phase of the micromotion and

1 - Since the MTI filter is a linear filter and noise and clutter are indepenent processes.

ψ_i is the initial phase relative to the target range. If I shows total number of scatterers inthe range under test, the reflected signal result from the combination of all target components can be written as

$$\mathbf{s}[\mathrm{n}] = \sum_{\mathrm{i}=1}^{\mathrm{I}} \mathbf{s}_{\mathrm{i}}[\mathrm{n}].$$

Notice that, due to the requirement of the coherency in a CPI, main parameters of the radar system (e. g. operating frequency, intrapulse coding, etc.) will not change within this interval. Consequently, the target amplitude is assumed to be constant and its change is CPI to CPI (Swerling I and III), but varies dues to components of the target, mathematically, $\mathrm{a_i}(\mathrm{n}) = \gamma_{\mathrm{i}}$. Therefore,

$$\boldsymbol{s}[n] = \sum_{i=1}^{I} \gamma_i e^{\{\jmath a_i n^2 + \jmath 2\pi\beta_i n + \jmath 2\pi\zeta_i \cos(2\pi\mu_i n + \theta_i) + \jmath\psi_i\}} \quad (4)$$

where probability density function of the unknown variable γ_i, is Rayleigh with the assumption of Swerling I for amplitude fluctuation of the target, while it is chi-square if we assume Swerling III for the amplitude fluctuation. Notice that the model provided in (4) will be simplified to the model presented in [13], if we assume the chirp rate $\mathrm{a_i} = 0$. Also, neglecting the micro-Doppler signature, the model will simplifed to some of chirplets [30].

All the proposed classification algorithms consist of at least two stages; signal analysis and feature extraction. In the next section, two important method for signal analysis is explained.

III. Proposed Method

Signal analysis is concerned with the estimation of a signal whose TF characteristics are in the desired fashion. The advantage of specifying the behavior of the signal to be analyzed in TF plane is that its characteristics can be time-variant or non-stationary, which is not available either in the time or frequency-domain representation [19]. Further, the modeling and description of a nonstationary signal jointly in time and frequency can be better understood by Fourier transforming the short segments of the signal [31]. This information has motivated many papers (e. g., [6]–[9], [11], [13]–[16]) to process the micro-Doppler in joint TF domain.

A. STFT

The STFT of the micro-Doppler signature is [15]

$$\xi(\omega, k;\ \Sigma) = \sum_{n=0}^{N-1} s[n] h_{\Sigma}^{*}[n-k] e^{-\jmath\omega n} \quad (5)$$

where $k = 0, \ldots, K-1, \omega$ is the angular frequency and $\mathrm{h}(.)$ is the smoothing window of the fixed length Σ. It is obvious that due to fixed window length in STFT, it does not provide good resolution at all the frequencies. In practice, the procedure for computing STFTs is to divide a longer time signal into shorter segments of equal length and then compute the K-point FFT separately on each shorter segment. The magnitude squared of the STFT yields the spectrogram of the function.

B. GLCT

The GLCT uses a different representation of the signal components, which in this case are called Chirplets [12], [19]–[23]. This transform considers time shifting, frequency shifting, scaling, chirping in time, and chirping in frequency. The GLCT of the micro-Doppler is [19],

$$\Gamma(\omega, k, \alpha, \psi;\ \Sigma) = \sum_{n=0}^{N-1} s[n] h_{\Sigma}^{*}[n-k] e^{-\jmath\omega\left[\frac{\alpha}{2}(n-k)^2 + \omega(n-k) + \psi\right]} \quad (6)$$

where α is the chirp rate and ψ is the initial phase with ω as the angular frequency and $\mathrm{h}(.)$ as the smoothing window of length Σ. Analogous to STFT, GLCT originates from a mother chirplet, which is basically a window function and can be modified to get the desired effects in TF representation. In the TF plane, we are mainly interested in the magnitude and hence if we consider the absolute value of the GLCT, we get

$$\Gamma(\omega, k, \alpha, \psi;\ \Sigma) = \sum_{n=0}^{N-1} s[n] h_{\Sigma}^{*}[n-k] e^{-\jmath\omega\left[\frac{\alpha}{2}(n-k)^2 + \omega(n-k) + \psi\right]} = \sum_{n=0}^{N-1} s[n] h_{\Sigma}^{*}[n-k] e^{-\jmath\frac{\alpha}{2}n^2} e^{\jmath\alpha nk} e^{-\jmath\omega n} \equiv \Gamma(\omega, k, \alpha;\ \Sigma) \quad (7)$$

which shows the initial phase ψ will not appear in the magnitude of GLCT. It is worth noting that GLCT equals STFT when α is set to 0. In terms of the joint TF resolution, for a gaussian window of length Σ, the minimum frequency bandwidth that can be achieved is $\frac{1}{\Sigma}$. This is the frequency bandwidth introduced due to the window. Since GLCT is a generalization of STFT, it can only perform as well as the STFT does for a stationary signal. Now, we shall see how the chirp rate α affects the frequency resolution of the GLCT.

In the next section we introduce a family of geometric moments, namely Zernike Moment (ZM) to extract invariant features from the TF representation.

C. Pseudo Zernike Moments

The pseudo ZMs can be defined as a set of complete complex orthogonal[1] basis functions based on Zernike polynomials that are square intergrable and defined over the unit circle. Zernike polynomials are used to characterize

1 -Orthogonality here means that there is no redundancy or overlapping of information between the moments.

higher-order errors observed in interferometric analyses. In optometry and ophthalmology, Zernike polynomials are used to describe aberrations of the cornea or lens from an ideal spherical shape, which result in refraction errors. Let a piecewise continuous function $f(x, y)$ (with bounded support) be the intensity function of a real TF image in Cartesian coordinates. The regular moments of $f(x, y)$ can be defined as

$$\mu_{p,q} = \int_x \int_y x^p y^q f(x,y) dxdy \tag{8}$$

where $(p, q) \in Z_+$ and $p+q$ is the degree of the moments. Note, (8) represents the projection of $f(x, y)$ on monomial $x^p y^q$. Since $x^p y^q$ is not an orthogonal set, $\mu_{p,q}$ are not independent moments. When the moments are generated from a set of orthogonal polynomials, we refer to these polynomials as pseudo Zernike polynomials. The pseudo Zernike polynomials are a set of complex polynomials described as

$$z_n^m(r,\theta) = \rho_n^m(r)\exp(jm\theta) \tag{9}$$

where $r \equiv \sqrt{x^2 + y^2}$ and $\theta \equiv \tan^{-1}(\frac{y}{x})$ are the length and angle of the position vector of a point (x, y) w.r.t. the center of the image, respectively, $n \in Z$ is the degree of the polynomial with frequency m, i.e., $m \in [-n; +n]$, and

$$\tilde{n}_n^m(r) \equiv \sum_{k=0}^{n-|m|} \frac{(-1)^k (2n+1-k)! r^{n-k}}{k!(n+|m|+1-k)!(n-|m|-k)!} \tag{10}$$

is the radial polynomial. When defined over a unite circle, i.e., $r \le 1$, the pseudo Zernike polynomials exhibit orthogonality, i.e.,

$$\int_0^{2\pi} \int_0^1 [z_n^m(r,\theta)]^* \left[z_{n'}^{m'}(r,\theta)\right] r dr d\theta = \frac{\pi}{n+1} \sigma_{nn'} \sigma_{mm'} \tag{11}$$

Where $\sigma_{ii'}$ is the Kronecker delta function. Now, the pseudo ZM can be obtained by projecting the image onto the pseudo Zernike polynomials as

$$a_n^m = \frac{n+1}{\pi} \int_0^{2\pi} \int_0^1 [z_n^m(r,\theta)]^* f(r,\theta) dr d\theta \tag{12}$$

Where $f(r,\theta) = f(x,y)\,|_{x=r\cos\theta, y=r\sin\theta}$.

D. Target Classification

Classification is a technique where we categorize data into a given number of classes. The main goal of a classification problem is to identify the category/class to which a new data will fall under. In classical machine learning, there are several algorithms including Logistic Regression, Naive Bayes, Stochastic gradient descent, k-Nearest Neighbors (k-NN), Decision Tree, Random forest, and Support vector machine, well-known as the powerful classifiers. In logistic regression, the probabilities describing the possible outcomes of a single trial are modeled using a logistic function. Logistic regression is most useful for understanding the influence of several independent variables on a single outcome variable. This method works only when the predicted variable is binary, assumes all predictors are independent of each other, and assumes data is free of missing values. Naive Bayes algorithm based on Bayes' theorem with the assumption of independence between every pair of features. Naive Bayes classifiers work well in many real-world situations such as document classification and spam filtering. This algorithm requires a small amount of training data to estimate the necessary parameters. Naive Bayes classifiers are extremely fast compared to more sophisticated methods. However, this algorithm is known to be a bad estimator. Stochastic gradient descent is a simple and very efficient approach to fit linear models. It is particularly useful when the number of samples is very large. It supports different loss functions and penalties for classification. However, this algorithm requires a number of hyper-parameters and it is sensitive to feature scaling. k-NN simply stores instances of the training data and the classification is computed from a simple majority vote of the k nearest neighbors of each point. This algorithm is simple to implement, robust to noisy training data, and effective if training data is large. However its computation cost is high as it needs to computer the distance of each instance to all the training samples. Decision tree produces a sequence of rules that can be used to classify the data. This method is simple to understand and visualize, requires little data preparation, and can handle both numerical and categorical data. However, Decision tree can be unstable because small variations in the data might result in a completely different tree being generated. Random forest classifier is a meta-estimator that fits a number of decision trees on various sub-samples of datasets and uses average to improve the predictive accuracy of the model and controls over-fitting. The sub-sample size is always the same as the original input sample size but the samples are drawn with replacement. Random forest classifier is more accurate than decision trees in most cases, however, it has slow real time prediction, difficult to implement, and complex algorithm. Finally, Support Vector Machine (SVM) is a representation of the training data as points in space separated into categories by a clear gap that is as wide as possible. New examples are then mapped into that same space and predicted to belong to a category based on which side of the gap they fall. This method is effective in high dimensional spaces and uses a subset of training points in the decision function so it is also memory efficient.

A block diagram of the whole classification algorithm is shown in Fig. 1. The reflected signal from the target first will face with some pre-processing such as down

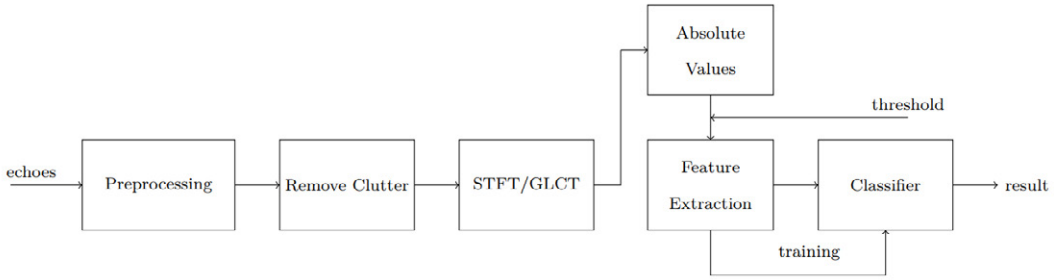

Fig. 1: Block scheme of the classifier algorithm

conversion and match filtering. Then, the clutter suppression block will improve SCR using a high-pass filter (MTI filter). TF image is the next step which can be provide either with STFT or GLCT. The magnitude then will be calculated and finally, the feature vector will extracted trough pseudo ZMs. A typical classifier can be used to determine type of target. Notice that the use of ZMs [11], [13] allows the introduction of important characteristics in the representation of a micro-Doppler signature, in order to fit different requirements. In particular translational invariance allows the unique identification of targets with different main Doppler shifts but belonging to the same class.

Further, the k-NN is regarded as the most effective classifier since it computes the distances between testing sample and all training samples, and then chooses the target type corresponding to the minimum distance as the type of the testing sample. According to the Fig. 1, there are two stages, i.e., training stage and classification stage, in the classification procedure. The training stage is done when the training sets have infinity Signal to Noise Ratio (SNR).

IV. Experimental Results

In this section, we illustrate effectiveness of STFT and GLCT in classification rate of the classifier algorithm. We assumed an X-band radar system[1]with bandwidth B =1MHz and Pulse Repetition Frequency PRF =5kHz. We consider coherent interval time TCPI = 0.8192s which[2] means 4096 pulses in a CPI. As to the TF analysis, we use a sampling rate[3] 5kHz, window size 256 points with overlap 50%. Also a smoothing hamming window is used for both STFT and GLCT. The primary components of the reflected signal, depending on the type of target can be torso, legs, arms, blade, rolling tire, etc. According to the model provided in (4), we have plenty of parameters to characterize each target amplitude fluctuation, movement and micro-motion including, γ, α, β, ζ, μ, θ and ψ. In order to observe micro-Doppler effect, we fix the parameters α, β, θ, ψ which are not directly related to the micro-Doppler motion.

Table I : Target Parameters

	σ_γ^2	α	β	σ_ζ^2	σ_μ^2	θ	ψ
Human	3	100	500	1	20	30	80
Animal	2	100	500	1	10	30	80
Drone	5	100	500	1	50	30	80
Vehicle	1	100	500	1	1	30	80

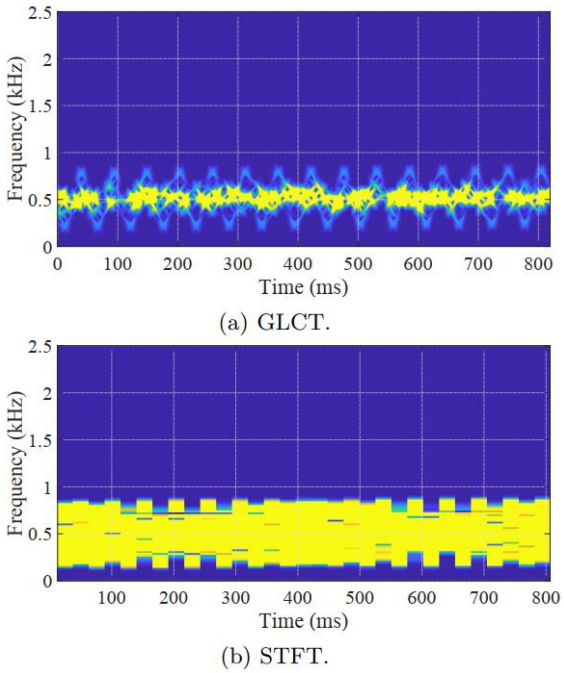

Fig. 2: Human Signature.

This assumption means that we have considered a unify Doppler frequency and chirp rate for all the targets which makes the classification task more strict. Also, Swirling I is assumed target amplitude fluctuation with mean 10 for all the targets but variances[4] as specified in TABLE I. The parameter ζ, μ which show the amplitude and frequency of the micro-motion, respectively, are considered as unknown zero-mean Gaussian random variables with variance as depicted in TABLE I. Further, in all cases, number of total components for every target assumed to be I = 5, we used Zernike moment until order 11 for the feature vector and number of Chirplets in GLCT are assumed to be 7.

In Fig. 2 the GLCT and STFT of the noise-free signal

1 -We assume a low-resolution radar system to show effectiveness of the proposed classification algorithm for this system.

2 Note that CPI time is the interval that one coherently integrate the reflected signal from the target. Assuming PRF = 5000Hz,in TCPI = 0.8192 the received 4096 pulses can obtain 36.12 dBprocessing gain. Decreasing the CPI time, cause to reduction inprocessing gain, and consequently affect the classification rate.

3 - Which is equal to the PRF

4 Notice that σ_z^2 shows the variance of the parameter z in TABLE I.

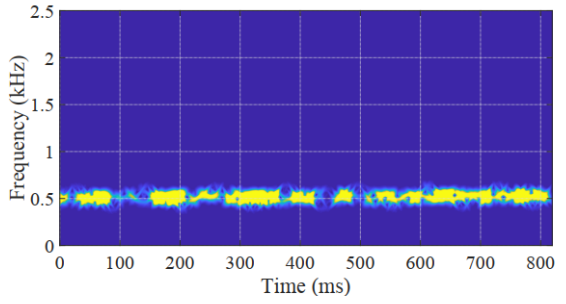

(a) GLCT.

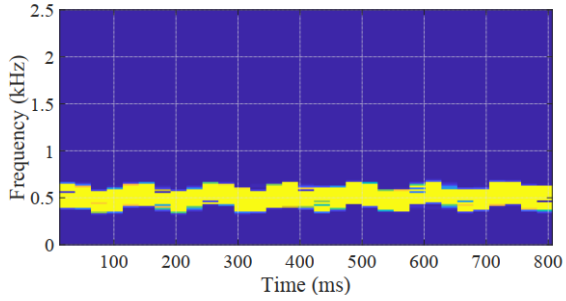

(b) STFT.

Fig. 3: Animal Signature.

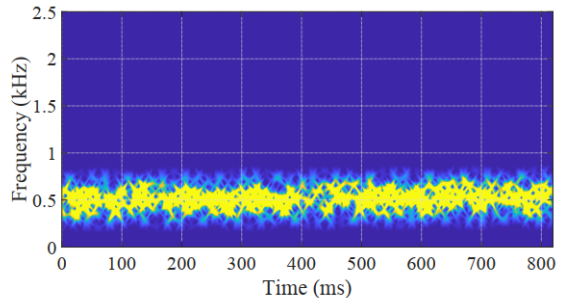

(a) GLCT.

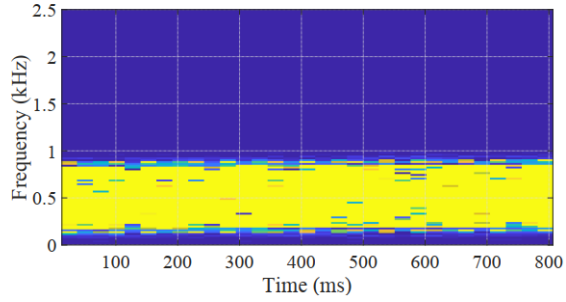

Fig. 4: Drone Signature.

for a person walking with a constant velocity is depicted. The signal reflected from the torso will have a constant Doppler shift while signal reflected from the components of the target, swinging legs and arms will be modulating at cadence frequency, which is the step or leg swing rate. In general, the arms and legs will have the same periodicity since the arms swing to counterbalance the legs. The shorter, thinner legs of the animals must have a narrower and sharper Doppler pattern compared to the broader pattern for the person which are depicted in Fig. 3. In the other hand, drone with the rotating blades spread more Doppler frequency as illustrated Fig. 4. Finally, Fig. 5 shows the TF analysis of the

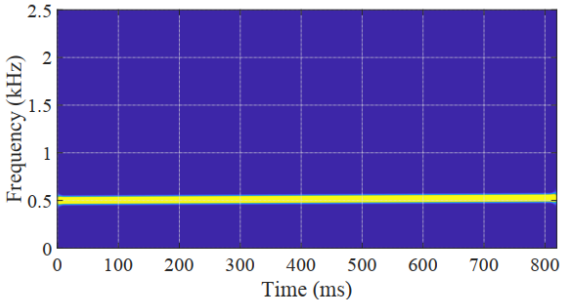

(a) GLCT.

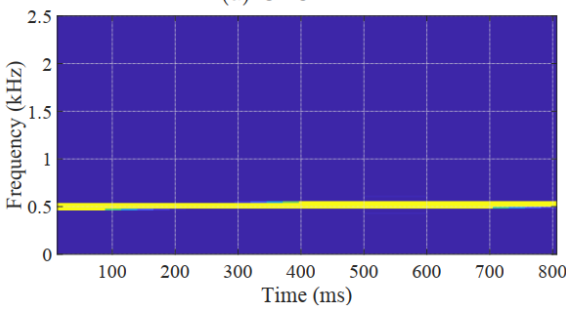

(b) STFT.

Fig. 5: Vehicle Signature.

reflected signal of the vehicle. As its observable in TF images of the different presented Figures, the more compatible GLCT extract the components more accurately than STFT which affects the classification rate. Fig. 6 compare four classes of targets in TCPI when SNR varies from -10dB to +30dB. The classification rate is averaged over 100 trials in each SNR. The Zernike vector extracted form the noise free signal is used as the training set in k_{NN} classifier for each target. When a new sample arrives, k_{NN} finds the k neighbors nearest to the new sample from the training space based on some suitable similarity or distance metric. The plurality class among the nearest neighbors is the class label of the new sample. As illustrated in Fig. 6, animal, personnel, drone and vehicle behave are classified better when GLCT is used for feature extraction instead of STFT. The difference in classification rate is more significant in low SNRs. The results show that extending the analysis domain to shear, scale, translation, etc., which has led to the evolution improves the performance of an equal classifier.

A. Comparison with the counterparts

In [15], employing low-resolution radar systems, a micro-Doppler feature extraction based on time frequency spectrogram is proposed to categorize ground moving targets into three types: single walking person, two people walking, and a moving wheeled vehicle. The main innovation of this paper is the definition of a novel 3-dimensional micro-Doppler feature vector extracted from the time-frequency spectrograms to represent the micro-motion characteristics of single walking person, two people walking and a moving wheeled vehicle. In this paper, the 3-dimensional features are extracted based on:

- Feature 1: the variance of the time-frequency spectrogram.

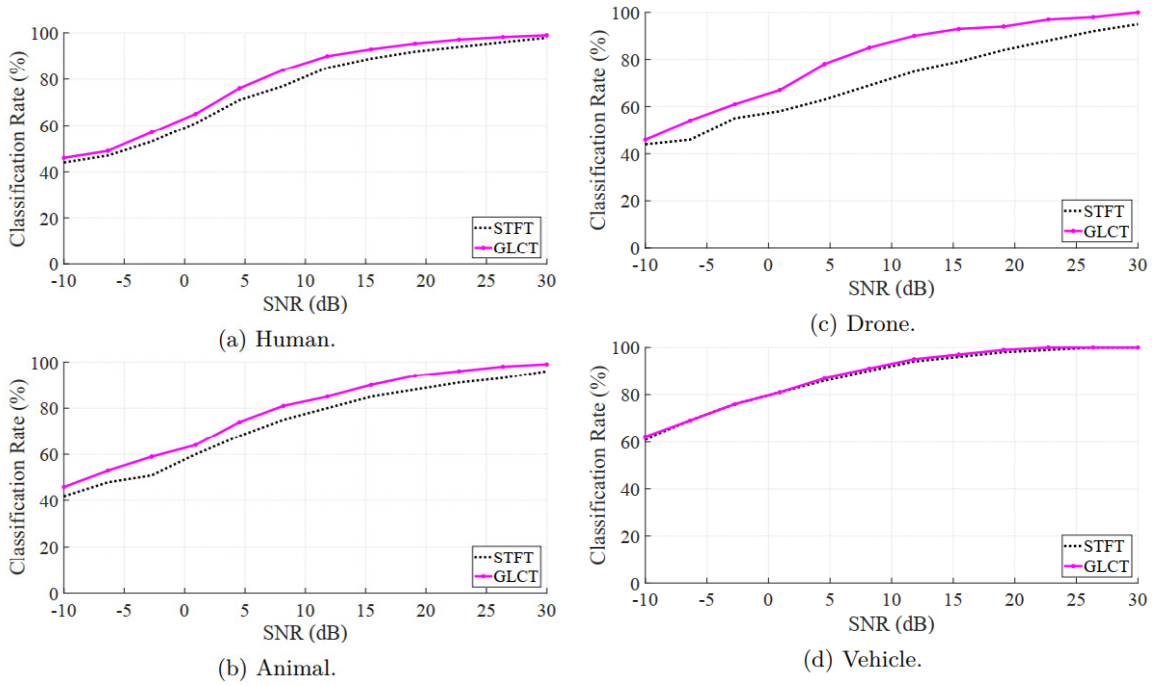

Fig. 6: Classification rate of four-class problem in different SNRs.

TABLE II: Comparison between the performance of the proposed method and that of presented by the counterparts.

	Classification Rate (%)	Algorithm	Reference
Vehicle	98.33	3-D	[15]
Human	91.67	3-D	[15]
Vehicle	92.75	Krawtchouk	[17]
Human	88.13	Krawtchouk	[17]
Vehicle	93.64	2D PCA	[9]
Human	90.79	2D PCA	[9]
Vehicle	98.12	GLCT	Proposed
Human	97.65	GLCT	Proposed

• Feature 2: the bandwidth of the target's Doppler modulations in the time-frequency spectrogram.
• Feature 3: the variance of the frequencies corresponding to the largest values in each column of the time-frequency spectrogram.

Then, to perform the classification, the extracted features in the training stage are utilized to train a SVM which is then used to determine the category of each test acquisition. The results of the proposed method in this paper is reported in TABLE II. In [17], a similar problem for target classification in Synthetic Aperture Radar (SAR) is considered by using the weighted Krawtchouk polynomials. The performance of the proposed method in classification of the vehicle is reported in TABLE II. Note that the extracted features are normalized and then trained to the k-NN classification algorithm. Finally, in [9] the use of principle component analysis (PCA) and 2-D PCA is proposed as the data driven feature extraction approaches. The feature extraction is taken over the spectrogram of the raw data. The results are reported in TABLE II. Note that all the comparisons all done with a noiseless raw data. According to TABLE II, we can see the proposed algorithm of this paper can obtain a better performance in comparison with the counterparts. Indeed the more accurate estimation of the time-frequency representation of the reflected signal, lead to a better performance.

TABLE III: Comparison between the run-time (s) of the proposed method and that of presented by the counterparts.

Method	[15] 3-D	[17] Krawtchouk	[9] 2D PCA	Proposed GLCT
Vehicle	0.74	0.81	1.32	0.83
Human	0.67	0.83	1.29	0.84

B. Computational Complexity

In the sequel, a comparison between the run-time (s) for classification of the reflected signal of one CPI, i. e., 4096 pulses, of the different methods proposed in [9], [15], [17], and that of proposed in this paper. The reported values are obtained with a standard PC with Intel (R) Core(TM) i7-600U CPU@ 2.80GHz with installed memory (RAM) 8.00 GB. According to TABLE III, in these examples, the computational complexity of the proposed method and Krawtchouk [17] are relatively in a same order. Notice that, even-though [15] has lower computational complexity, its performance is very sensitive to the predefined values for Doppler and bandwidth spread of the targets.

C. Effect of the Swerling Models of the Classification Performance

The Swerling target models give the statistical model for the radar cross-section (RCS) of a given object, i.e., amplitude of the reflected signal. Indeed, using the Swerling models the amplitude of the reflected signal assumed to be a random variable and its distribution is modeled in a family of the chi-

squared distributions [10]. Different cases of the Swerling models are briefly described below:

• **Swerling I**: This case describes a target whose magnitude of the backscattered signal is relatively constant during the dwell time. It varies according to a Rayleigh probability density function. The radar cross-section is constant from pulse-to-pulse, but varies independently from scan to scan.

• **Swerling II**: The Swerling II target is similar to Swerling I, using the same equation, except the RCS values changes faster and varies from pulse to pulse additionally. The Swerling cases I and II applies to a target that is made up of many independent scatterers of roughly equal areas like airplanes. However, in Swerling case II there is no rotating surveillance antenna but a focused onto a target tracking radar.

• **Swerling III**: This case describes a target whose magnitude of the backscattered signal is relatively constant during the dwell time. It varies according to a Chi-square probability density function with twodegrees of freedom. The radar cross-section is constant from pulse-to-pulse, but varies independentlyfrom scan to scan.

• **Swerling IV**: The Swerling case IV is similar to Swerling III, but the RCS varies from pulse to pulse rather than from scan to scan.

Note that in general, the cases I and III apply for search radars [10], which is the case we considered in this paper. Indeed pulse-to-pulse fluctuations happens when there is a change in the coherence time of the radar system, i.e., changing the carrier frequency, transmitting phase, etc. The fluctuation loss depends on the probability of detection and for the radar that is assumed in this paper, at $P_d = 0.9$ is shown in Fig. 7. In ground surveillance radar systems (the radar of this paper), during a coherent pulse interval (CPI), targets remain within a resolution cell. Also, as the need for coherent processing, the main parameters of the system like frequency, phase or pulse repetition interval (PRT) remains fixed. As a result, within one CPI the amplitude of the reflected signal is a random variable that can varies scan-to-scan. This means that in each CPI, the received Signal-to-Noise-Ratio (SNR) of the received signal will changes. Consequently, since the classification rate is dependent to the received SNR values, the performance will changes accordingly. In Fig. 8, performance of the proposed GLCT algorithm under Swerling models I and III is depicted. A comparison between this Figure and Fig. 6 of the paper indicates that the classification rate decreased considering the Swerling models. As expected, the loss in classification rate for Swerling III is less than that of Swerling I.

V. Conclusion

In this paper, the chirplet transform is applied to extract micro-Doppler features from different target reflections. Precisely, we have shown the micro-Doppler signature of the reflected signal in a radar system can be analyzed more accurately by using GLCT rather than STFT. Hence, in the low SNR cases the micro-motion components are contaminated by the noise and more accurate TF representation plays more significant role in the target classification procedure. Indeed, we have used ZMs feature vector to reach high capability of recognition.

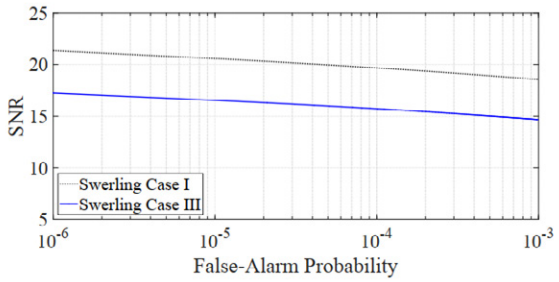

Fig. 7: Fluctuation loss for Swerling cases I and III.

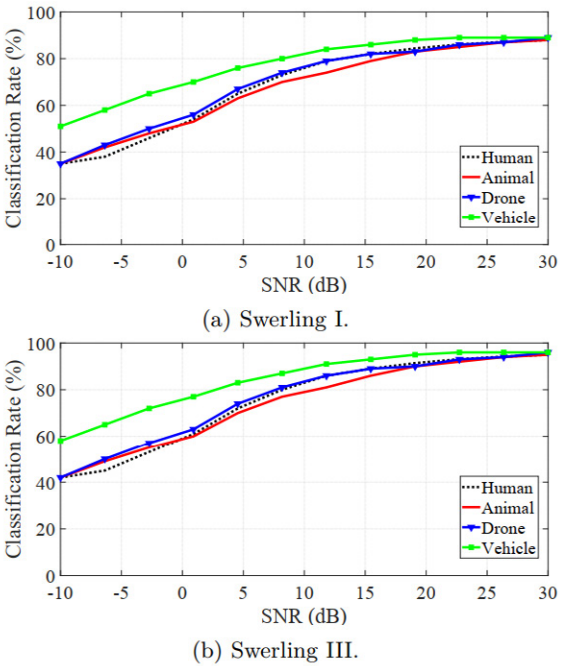

Fig. 8: Performance of the proposed GLCT algorithm under different Swerling models.

References

[1] W. L. Melvin and J. A. Scheer, Principles of modern radar.SciTech Publishing, 2014.

[2] G. Zhao, Y. Fu, L. Nie, and Z. Zhuang, "Imaging and micro Doppler analysis of vibrating target in Multi-Input-Multi Output synthetic aperture radar," IET Radar, Sonar Navigation, vol. 9, no. 9, pp. 1360–1365, 2015.

[3] X. Y. Pan, J. Liu, L. T. Xu, X. Ai, Q. Xie, B. Yu, andC. Li, "Extraction of micro-Doppler frequency from HRRPs of rotating targets," IEEE Access, vol. 5, pp. 26162–26174, 2017.

[4] L. Li, Z. Liu, and T. Li, "Radar high resolution range profile recognition via multi-SV method," Journal of Systems Engineering and Electronics, vol. 28, pp. 879–889, Oct 2017.

[5] C. Bentes, D. Velotto, and B. Tings, "Ship classification in TerraSAR-X images with convolutional neural networks," IEEE Journal of Oceanic Engineering, vol. 43, pp. 258–266, Jan 2018.

[6] M. Alaee and H. Amindavar, "Chirplet-based target recognition using RADAR technology," in 2008 5th IEEE Sensor Array and Multichannel Signal Processing Workshop, pp. 451–454, July 2008.

[7] D. Tahmoush, "Review of micro-Doppler signatures," IET Radar, Sonar Navigation, vol. 9, no. 9, pp. 1140–1146, 2015. [8] D. P. Fairchild and R. M. Narayanan, "Multistatic micro Doppler radar for determining target orientation and activity

classification," IEEE Transactions on Aerospace and Electronic Systems, vol. 52, pp. 512–521, February 2016.
[9] W. Li, B. Xiong, and G. Kuang, "Target classification and recognition based on micro-doppler radar signatures," in 2017 Progress in Electromagnetics Research Symposium – Fall (PIERS - FALL), pp. 1679–1684, Nov 2017.
[10] M. Skolnik, Radar Handbook, Third Edition. Electronics electrical engineering, McGraw-Hill Education, 2008.
[11] M. Alaee, H. Amindavar, and A. M. Reza, "A new approach to moving terrestrial targets recognition using ground surveillance pulse Doppler RADARs," in 2008 IEEE Radar Conference, pp. 1–6, May 2008.
[12] S. G. Pelluri and T. V. Sreenivas, "Parameter estimation of a moving acoustic source: Linear chirplet transform vs wvd," in 2017 Twenty-third National Conference on Communications (NCC), pp. 1–6, March 2017.
[13] C. Clemente, L. Pallotta, A. D. Maio, J. J. Soraghan, and A. Farina, "A novel algorithm for radar classification based on Doppler characteristics exploiting orthogonal pseudo-Zernike polynomials," IEEE Transactions on Aerospace and Electronic Systems, vol. 51, pp. 417–430, January 2015.
[14] B. Tekeli, S. Z. Gurbuz, and M. Yuksel, "Information-theoretic feature selection for human micro-Doppler signature classification," IEEE Transactions on Geoscience and Remote Sensing, vol. 54, pp. 2749–2762, May 2016.
[15] L. Du, L. Li, B. Wang, and J. Xiao, "Micro-Doppler feature extraction based on time-frequency spectrogram for ground moving targets classification with low-resolution radar," IEEE Sensors Journal, vol. 16, pp. 3756–3763, May 2016.
[16] A. K. Singh and Y. H. Kim, "Automatic measurement of blade length and rotation rate of drone using w-band micro-Doppler radar," IEEE Sensors Journal, vol. 18, pp. 1895–1902, March 2018.
[17] C. Clemente, L. Pallotta, D. Gaglione, A. D. Maio, and J. J. Soraghan, "Automatic target recognition of military vehicles with krawtchouk moments," IEEE Transactions on Aerospace and Electronic Systems, vol. 53, pp. 493–500, Feb 2017.
[18] G. Yu and Y. Zhou, "General linear chirplet transform," Mechanical Systems and Signal Processing, vol. 70-71, pp. 958 – 973, 2016.
[19] G. Yu and Y. Zhou, "General linear chirplet transform," Mechanical Systems and Signal Processing, vol. 70-71, pp. 958 – 973, 2016.
[20] A. Taebi and H. A. Mansy, "Analysis of seismocardiographic signals using polynomial chirplet transform and smoothed pseudo wigner-ville distribution," in 2017 IEEE Signal Processing in Medicine and Biology Symposium (SPMB), pp. 1–6, Dec 2017.
[21] U. Singh and S. N. Singh, "Detection and classification of power quality disturbances based on time–frequency-scale transform," IET Science, Measurement Technology, vol. 11, no. 6, pp. 802–810, 2017.
[22] X. Tu, Y. Hu, F. Li, S. Abbas, and Y. Liu, "Instantaneous frequency estimation for nonlinear fm signal based on modified polynomial chirplet transform," IEEE Transactions on Instrumentation and Measurement, vol. 66, pp. 2898–2908, Nov 2017.
[23] J. Sharma, V. Thakur, and S. D. Sharma, "Evaluation of time frequency tools for multi-component chirp signals," in International Conference on Signal Processing (ICSP 2016), pp. 1–6, Nov 2016.
[24] A. Krizhevsky, I. Sutskever, and G. E. Hinton, "Imagenet classifcation with deep convolutional neural networks," in Advances in neural information processing systems, pp. 1097– 1105, 2012.
[25] M. D. Zeiler and R. Fergus, "Visualizing and understanding convolutional networks," in European conference on computer vision, pp. 818–833, Springer, 2014.
[26] C. Szegedy, W. Liu, Y. Jia, P. Sermanet, S. Reed, D. Anguelov, D. Erhan, V. Vanhoucke, and A. Rabinovich, "Going deeper with convolutions," in Proceedings of the IEEE conference on computer vision and pattern recognition, pp. 1–9, 2015.
[27] Y. Kim and T. Moon, "Human detection and activity classification based on micro-Doppler signatures using deep convolutional neural networks," IEEE Geoscience and Remote Sensing Letters, vol. 13, pp. 8–12, Jan 2016.
[28] B. Vandersmissen, N. Knudde, A. Jalalvand, I. Couckuyt, A. Bourdoux, W. D. Neve, and T. Dhaene, "Indoor person identifcation using a low-power FMCW radar," IEEE Transactions on Geoscience and Remote Sensing, vol. 56, pp. 3941– 3952, July 2018.
[29] S. Deng, L. Du, C. Li, J. Ding, and H. Liu, "Sar automatic target recognition based on euclidean distance restricted autoencoder," IEEE Journal of Selected Topics in Applied Earth Observations and Remote Sensing, vol. 10, pp. 3323–3333, July 2017.
[30] Y. Lu, E. Oruklu, and J. Saniie, "Fast chirplet transform with fpga-based implementation," IEEE Signal Processing Letters, vol. 15, pp. 577–580, 2008.
[31] Q. Jiang and B. W. Suter, "Instantaneous frequency estimation based on synchrosqueezing wavelet transform," Signal Processing, vol. 138, pp. 167 – 181, 2017.

HOW TO CITE THIS ARTICLE

R. Amiri, A. Shahzadi, General Linear Chirplet Transform and Radar Target Classification, AUT J. Elec. Eng., 51(2) (2019) 113-122.

DOI: 10.22060/eej.2019.15276.5257